

Sonic Hedgehog-activated engineered blood vessels enhance bone tissue formation

Nicolas C. Rivron^{a,1}, Christian C. Raiss^a, Jun Liu^a, Anandkumar Nandakumar^a, Carsten Sticht^c, Norbert Gretz^c, Roman Truckenmüller^a, Jeroen Rouwkema^b, and Clemens A. van Blitterswijk^a

^aDepartment of Tissue Regeneration, MIRA Institute for Biomedical Technology and Technical Medicine, 7500AE, University of Twente, Enschede, The Netherlands; ^bDepartment of Biomechanical Engineering, MIRA Institute for Biomedical Technology and Technical Medicine, 7500AE, University of Twente, Enschede, The Netherlands; and ^cMedical Research Centre, Medical Faculty Mannheim, University of Heidelberg, Mannheim, Germany

Edited by Robert Langer, MIT, Cambridge, MA, and approved January 19, 2012 (received for review October 25, 2011)

Large bone defects naturally regenerate via a highly vascularized tissue which progressively remodels into cartilage and bone. Current approaches in bone tissue engineering are restricted by delayed vascularization and fail to recapitulate this stepwise differentiation toward bone tissue. Here, we use the morphogen Sonic Hedgehog (Shh) to induce the *in vitro* organization of an endothelial capillary network in an artificial tissue. We show that endogenous Hedgehog activity regulates angiogenic genes and the formation of vascular lumens. Exogenous Shh further induces the *in vitro* development of the vasculature (vascular lumen formation, size, distribution). Upon implantation, the *in vitro* development of the vasculature improves the *in vivo* perfusion of the artificial tissue and is necessary to contribute to, and enhance, the formation of *de novo* mature bone tissue. Similar to the regenerating callus, the artificial tissue undergoes intramembranous and endochondral ossification and forms a trabecular-like bone organ including bone-marrow-like cavities. These findings open the door for new strategies to treat large bone defects by closely mimicking natural endochondral bone repair.

angiogenesis | endochondral ossification | regenerative medicine | tissue engineering

Large bone defects with interfragmentary spaces and mobility regenerate via a highly vascularized callus which stabilizes the fracture site and progressively remodels into a bone organ (1). This callus is composed of a shell formed by intramembranous ossification (IO) and a core of highly vascularized fibrocartilage which undergoes endochondral ossification (EO) (1). The vascularization of the callus is quantitatively important and persists until the normal medullar, periosteal, and osseous blood supply is reestablished (2).

Current bone tissue engineering therapies often use bone-marrow-derived mesenchymal stem cells as an easily collectable and abundant source of cells with high expansion and chondrogenic/osteogenic differentiation capacity (3–4). However, these implants currently have limited survival and functionality due to a lack of vascularization (5). To overcome this problem, we previously demonstrated that endothelial cells can form a vascular network *in vitro* which can rapidly anastomose with the host vasculature upon implantation (6). Our data and others (7–9) suggest that such an engineered vasculature must rapidly develop and become perfused upon implantation to prevent the regression of capillaries (8), form functional blood vessels (6), and possibly contribute to the formation of new tissues. These results raised two important questions in vascular tissue engineering. First, does the *in vitro* development of the vasculature improve its *in vivo* functionality? Second, if this vasculature becomes functional *in vivo*, can it contribute to and enhance tissue formation?

Hedgehog (Hh) proteins act as archetypical morphogens regulating multiple processes during embryonic development. Hh signaling is relatively silent during homeostasis but reactivates during several adult regenerative processes, participates in neovascularization (10, 11–14), and in fracture healing (10–15).

Among the three human Hh genes (Sonic, Indian, and Desert Hedgehog), Sonic Hedgehog (Shh) is the most expressed, is essential for endothelial tube formation during vascular embryonic development (16), neovascularization upon adult trauma, and wound healing (12–14, 17–18).

Here, we reasoned that Shh can be used to promote the *in vitro* development of engineered blood vessels to improve endochondral bone repair. Our data demonstrate that Shh promotes the *in vitro* development of engineered blood vessels which resulted, *in vivo*, in an improved perfusion of the implants and an enhanced formation of mature bone via a combination of intramembranous and endochondral ossification.

Results

Endogenous Hedgehog Signaling Regulates Lumen Formation in an Engineered Vasculature.

The coculture of cellular aggregates of hMSC (92%) and huvEC (8%) supports the formation of a primitive three dimensional vascular network mainly composed of cord-like structures and including some lumens [optimized by us earlier (19–20)] (Fig. 1A). We previously demonstrated that these vascular structures do not become rapidly functional upon implantation possibly due to a lack of maturation (19–20). Consistent with a role of Hh during vascular tube formation (16), we found that an inhibition of the canonical Hh signaling pathway using cyclopamine (5 μ M), a Smo modulator (21) (day 0 to 12), impaired the formation of lumens (2-fold, $p = 0.002$, Fig. 1B and C). A partial inhibition from day 4 to 12 was sufficient ($p = 0.001$), which suggests a later role for Hh in the development of lumens (Fig. 1C). A genetic screen (day 12) revealed that cyclopamine stimulation significantly regulated 303 genes among which 58 are directly linked to hedgehog signaling or angiogenesis (Figs. 1D and E, Fig. S1). Cyclopamine treatment regulated two Hh inhibitors (GAS1 and RAB23, Fig. 1D) and the two Hh target signaling pathways Wnt and TGF (Fig. S1). Consistent with current knowledge on vascular lumen formation (22), expression of laminins ($\alpha 1, 3, 4, 5, \beta 2$) and integrins ($\alpha 2, 7, \beta 5$) were regulated (Fig. 1E) along with axon guidance molecules (ephrin $\alpha 1, \beta 1, 2$, semaphorins 3G, 5A, 6A, 6D) and cytoskeletal elements (Fig. S1). These results demonstrate a role for endogenous Hh activity in regulating the formation of vascular structures and lumens.

Exogenous Sonic Hedgehog Protein Induces Vascular Lumen Formation *In Vitro*.

We tested the potential for exogenous Shh to improve

Author contributions: N.C.R., N.G., R.T., J.R., and C.A.v.B. designed research; N.C.R., C.C.R., J.L., and A.N. performed research; N.C.R. and C.S. analyzed data; and N.C.R. wrote the paper.

The authors declare no conflict of interest.

This article is a PNAS Direct Submission.

Freely available online through the PNAS open access option.

¹To whom correspondence may be addressed. E-mail: nicolasrivron@gmail.com.

This article contains supporting information online at www.pnas.org/lookup/suppl/doi:10.1073/pnas.1117627109/-DCSupplemental.

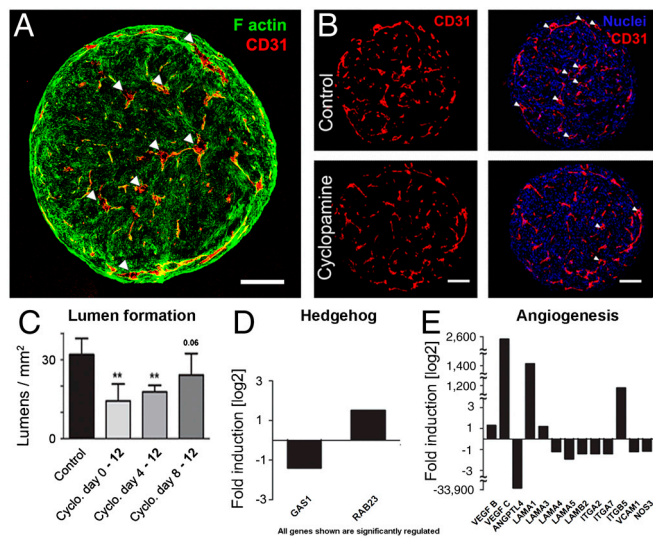


Fig. 1. Endogenous Hh activity regulates angiogenic genes and the formation of lumens. Multicellular aggregates of hMSC (92%) and huVEC (8%) aggregated in vitro and formed a primitive 3D vascular network including few lumens (day 12, lumens are indicated by arrow heads) (A). A specific pharmacological inhibition of the Hh pathway from day 0 and from day 4 using cyclopamine (5 μ M) decreased the number of lumens formed [(B) from day 0 to 12, (C), $n = 4$ sections \times 4 samples]. Genome-wide genetic screen on cyclopamine treated-multicellular aggregates revealed the regulation of two main inhibitors of the canonical Hh pathway (GAS1, RAB23) (D) and the regulation of angiogenic molecules (E). Laminins and integrins are of especially relevant to the formation of vascular lumens (E). All presented genes are significantly regulated as compared to vehicle-treated multicellular aggregates. VEGF: vascular endothelial growth factor; ANGPTL: angiopoietin-like; LAMA: laminin alpha; LAMB: laminin beta; ITGA: integrin alpha; ITGB: integrin beta; VCAM: vascular cell adhesion molecule; NOS: nitric oxide synthase. Errors bars are S.D. Scale bars are 100 μ m. ** signifies a p -value < 0.005 .

the formation of vascular lumens in vitro. A dose response assay in the physiological range (0.5–30 nM) (23) revealed a classical morphogen response inducing dose-dependent effects (Fig. 2A). 0.5 nM Shh induced a decrease in the number of lumens (3.25 lumens/mm², 13 lumens/mm² in the control, $p < 0.05$) while concentrations above 10 nM induced an increase in lumen formation up to 3.4 fold (44 lumens/mm², $p < 0.01$) (Fig. 2A). This resulted in a lumenization (opening) of the vascular structures covering up to 5.5% of the tissue area (7.5 fold increase at 10 nM; 0.73% at 0 nM and 0.13% at 0.5 nM, Fig. 2B). This effect was inhibited by cyclopamine (10 nM Shh, $p < 0.05$, Fig. 2C). A later stimulation (day 9 to 12) was sufficient, which correlated with the previous observation suggesting a later role for Shh in the development of lumens (Fig. 2D). The total vessel length area (total CD31+ area, mm²/mm²) was unchanged (Fig. S24) and the proliferation of huVEC in serum-free medium on 2D plastic decreased upon Shh stimulation (Fig. S2B). These results suggest that the increase in vascular lumens formation is not due to an increase in endothelial cell number. We concluded that Shh induced the formation of lumens independently of endothelial cell proliferation. Purmorphamine, a pharmacological activator of Hh pathway which shunts the Ptc receptor and directly unleashes Smo inhibition (24) induced a similar effect (day 8 to 12, Fig. 2E). We compared the effect induced by Shh to classical anti- and proangiogenic factors TGFB1, VEGF, and Ang1 (Fig. 2F). TGFB1 (10 ng/mL), an inhibitor of endothelial cell proliferation and motility (25), dramatically decreased lumen formation (TGFB1: 0.8 lumen/mm², control: 10.5 lumens/mm², $p < 0.05$). VEGF and Ang1 did not affect lumen formation. These findings correlate with previous observations that vascular networks formed in multicellular aggregates are not responsive to VEGF (26). The lumen

formation induced by Shh was reproduced using a commercially available hMSC population (Lonza Group Ltd.) (Fig. S3). These results suggest that exogenous Shh acts as a typical morphogen modulating vascular lumen formation based on its concentration.

Sonic Hedgehog Modulates the Distribution Profile of Vascular Lumens

To test the effect of exogenous Shh at the tissue level, we observed the distribution profiles of vascular lumen areas and their relative diameters (Fig. 2G and H). The untreated group (control group) and the group treated with 0.5 nM Shh developed uniformly small lumens with an average diameter of 26 μ m (Table S1) and an exponential distribution reflecting the prevalence of capillaries (Control group: Median lumen diameter = 21 μ m, 90th percentile = 35 μ m, Fig. 2G and H). In the group treated with 10 nM Shh, the distribution was normal, wider than in the control group ($p < 0.0003$, Table S1) and included lumens of middle and large diameters (10 nM Shh group: Median lumen diameter = 35 μ m, 90th percentile = 69 μ m). In contrast, the group treated with high Shh concentration (30 nM) had an average lumen diameter of 34 μ m, similar to the control ($p > 0.05$) with predominant small diameter lumens (30 nM Shh group: Median lumen diameter = 24 μ m, 90th percentile = 49 μ m, Table S1). These results suggest that, at a tissue level, exogenous Shh modulates the size and distribution profile of lumens. A concentration of 10 nM induced a maximal lumenization of the vascular structures (5.5% of the tissue area, Fig. 2A and B) and a normal, spread distribution of the lumen sizes reminiscent of a normal vascular hierarchy (Fig. 2G and H). These results are consistent with in vivo observations of Shh-induced neovascularization in ischemic hindlimb (11) and with the notion of morphogen.

Regulation of the Expression of Extracellular Matrix-Related Genes

We tested the possibility that, besides vascular development, Shh might regulate the production of a bone- and cartilage-related extracellular matrix (ECM). Using quantitative reverse transcriptase (qRT)-PCR to analyze mRNA levels, we observed that the stimulation of the coculture with Shh (10 nM, day 4 to 12) upregulated the expression of collagen type X (21 fold, $p = 0.04$, Fig. 3A), an effect inhibited by cyclopamine treatment (5 μ M, day 4 to 12). Other bone and cartilage ECM marker genes remained similar (Collagen I, collagen II, aggrecan) (Fig. 3C). We used histology and immunostaining to assess protein expression. Masson-Goldner staining revealed the presence of similar levels of collagen type I upon Shh treatment (green stain, Fig. S4). Neither the presence of collagen type II nor collagen type X was detectable by immunohistochemistry. We concluded that the mature proteins of collagen type II and X are either absent or present at very low levels in this coculture (Fig. 3B, Top) and not significantly modulated by Shh. The stimulation of the coculture with TGFB1 (10 ng/mL), an inducer of chondrogenic differentiation in hMSC, led to the production of collagen type II but to the concomitant disappearance of the CD31+ network (Fig. 3B, Bottom).

The Engineered Vasculature Increases Implant Perfusion in Vivo

To evaluate the potential in vivo functionality of the vasculature, implants composed of cellular aggregates and osteoinductive ceramic granules (27) in a collagen type I matrix were implanted subcutaneously in immuno-compromised mice. Cellular aggregates were formed with either hMSC alone (group 1); hMSC treated with 10 nM Shh (day 4 to 12, group 2); hMSC and huVEC (group 3); hMSC and huVEC treated with 10 nM Shh (day 4 to 12, group 4). Implants were first explanted and analyzed after 5 weeks. The engineered vasculature anastomosed with the host vasculature as demonstrated by the presence of erythrocytes in human CD31+ lumens (Fig. 4A). Implant perfusion was con-

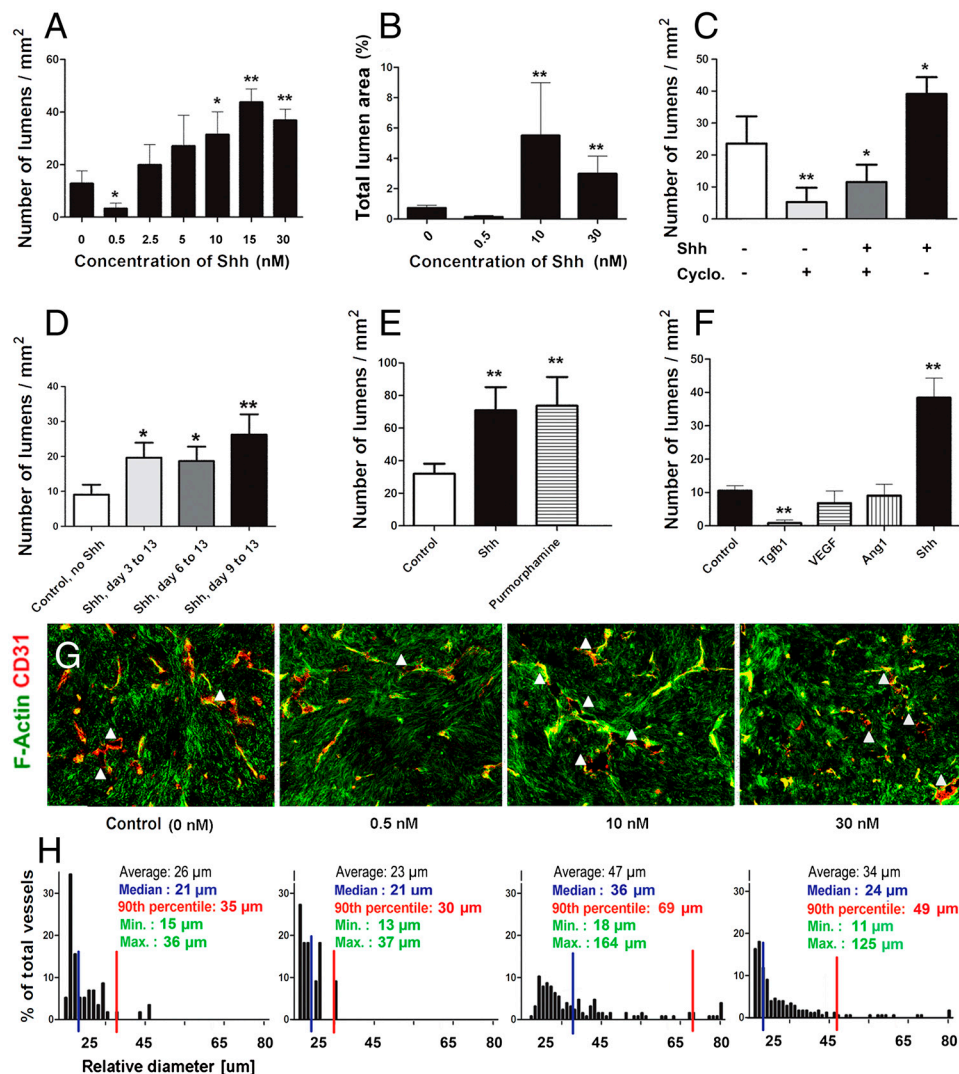


Fig. 2. Exogenous Shh improves the in vitro development of the vascular network. Multicellular aggregates treated with a physiological range of concentrations of Shh (0–30 nM) developed a typical morphogen response which either decreased (0.5 nM) or increased (10–30 nM) the number of vascular lumens (A). This resulted in a total lumen area covering up to 5.5% of the tissue area (10 nM) (B). The Shh-induced formation of lumens was further inhibited by cyclopamine (C). A later stimulation between day 9 and 12 was sufficient to increase the number of lumen (D) and was similarly induced by purmorphamine, a known pharmacological activator of the canonical Hh pathway (E). Classical direct effectors of the angiogenic cascade (TGF, VEGF, Ang1) did not increase the number of lumens formed (F). (G–H) The physiological range of concentrations of Shh affected differently the size-distribution of lumens [white arrow heads in (G) indicate lumens]. A wider, normal distribution typical of the vascular tree only formed at a concentration of 10 nM (see also Table S1). Aggregates treated with 0, 0.5, and 30 nM Shh had an exponential distribution with prevalent small lumens (G, H). $n = 4$ sections \times 4 samples for each experiment. Errors bars are S.D. * signifies a p -value <0.05 , ** a p -value <0.005 .

firmed by the injection of fluorescent lectin in the tail vein of the mice which overlapped with human CD31+ cells (Fig. 4B). Implants with an engineered vasculature (group 3) were more perfused as compared to implants without an engineered vasculature (group 1: 9 lumens/mm², group 3: 23 perfused lumens/mm², 5 mice, $p = 0.014$, Fig. 4C). The activation of the engineered vasculature using Shh (group 4) further improved implant perfusion,

resulting in a total density of 41 perfused lumens/mm² ($p = 0.02$, Fig. 4C). This vascular density is typical of highly vascularized tissues (6). Engineered blood vessels can be unstable, prone to remodeling and regression in vivo (8). Here, we observed that (i) cord-like (nonlumenized) structures present in vitro were absent after implantation (Fig. 4A and Fig. S5) and (ii) the density of lumens formed in vitro correlated with the density of lumens perfused in vivo (Fig. 2A and 4C). These results suggest that lumenized vessels have a more stable, functional phenotype and promote higher perfusion than cord-like structures upon implantation. This correlates with recently published observations that implanted vessels enhance implant perfusion partly via the recruitment of host-derived blood vessels (9). In vascularized implants, perfused blood vessels were derived for 60% \pm 3% from the mice (hCD31-) and for 40% \pm 3% from the implanted huVEC (hCD31+). Part of the capillaries were positive for the pericyte marker smooth muscle actin (Fig. S6), an observation consistent with the pericyte heterogeneity of the vascular bed (28).

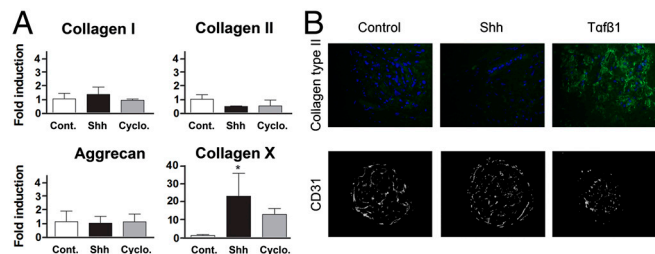


Fig. 3. Shh does not regulate the formation of cartilage or bone extracellular matrix. (A) Quantitative RT-PCR for collagen I, collagen type II, aggrecan, and collagen X showed that Shh stimulation (10 nM) regulated collagen type X mRNA (21 fold up, $p = 0.04$) without affecting collagen type I, collagen type II and aggrecan mRNA levels. $n = 3$, errors bars are S.D. The presence of collagen type I proteins was confirmed (see Fig. S4). (B) Neither the presence of collagen type II and X proteins was detectable by immunofluorescence (top row, collagen type II). The induction of a collagen type II cartilage ECM using TGF β 1 (10 ng/mL) resulted in the concomitant disappearance of the CD31+ network (bottom row, see also Fig. 2F). * signifies a p -value <0.05 .

Tissue Engineered Implants Recapitulate Intramembranous and Endochondral Ossification. After 5 weeks, a cartilage tissue aligned the inner part of the implants. This cartilage included round cells in large lacunae surrounded by proteoglycans (Alcian blue positive, Fig. 4D and E). Pericellular collagen type X, an extracellular matrix specific of hypertrophic cartilage (Inset, Fig. 4E), aligned the newly formed bone osteoids as expected during the process of EO

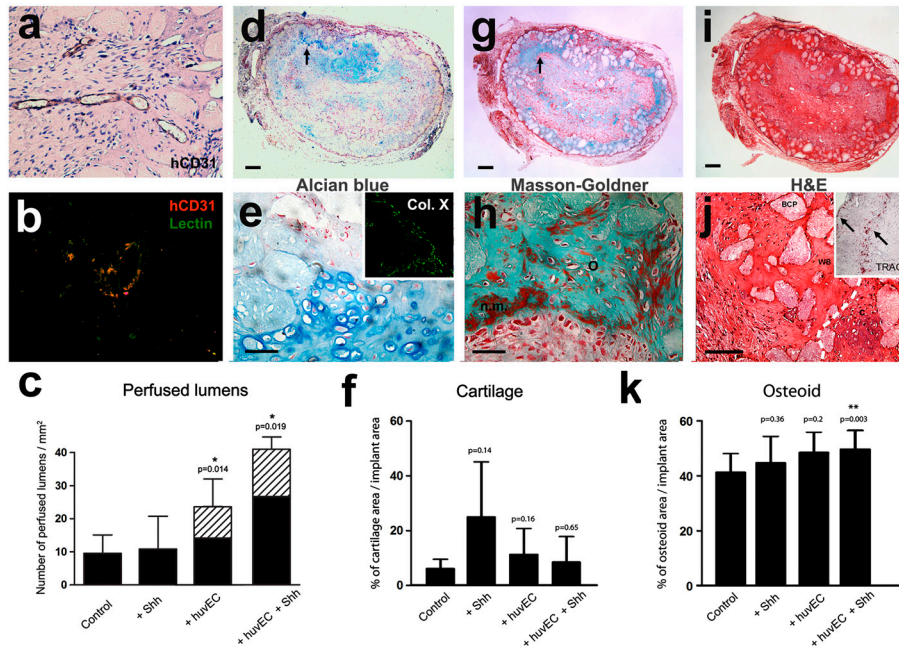


Fig. 4. Implants recapitulate endochondral ossification and engineered blood vessels enhance implant perfusion. Implants composed of cellular aggregates with osteoinductive ceramic particles were placed subcutaneously in mice, explanted, and analyzed after 5 weeks. Cellular aggregates were formed with hMSC (group 1, control group), hMSC stimulated with 10 nM Shh (group 2), hMSC with huVEC (group 3), or hMSC with huVEC stimulated with 10 nM Shh (group 4) (A–C) Functional perfusion of the engineered blood vessels. (A) Following implantation, human CD31+ lumens included erythrocytes and (B) were perfused by fluorescently labeled lectin injected into the mouse tail vein. (C) Shh-activated engineered blood vessels increased implant perfusion from 9 perfused lumens/mm² to 41 perfused lumens/mm² (Paired Student *T*-Test, $n = 5$, $p = 0.019$). 40–43% of the total perfused blood vessels were human (dashed area). (D–K) Formation of skeletal tissues. (D) A cartilage tissue formed, including round cells in large lacunae surrounded by proteoglycans (Alcian blue positive). (E) The cartilage tissue was partly hypertrophic (collagen type X, insert in E) and covered 5–25% of the implant area (F, n.s. between the four groups, paired Student *T*-Test, $n = 5$). (G–H) Bone osteoids formed at the periphery of the osteoinductive particles and at the interface with the cartilage tissue (Masson-Goldner staining, bone-cartilage interface is shown with black arrows D, G). (H) Osteoids included red, freshly secreted, nonmineralized matrix (in H: o is osteoids, n.m. is nonmineralized matrix). (I, J) Cartilage tissue aligned the bone osteoids (haematoxylin-eosin staining (J: c is cartilage, wb is woven bone, dashed white line delimits cartilage-osteoids interface). Lines of osteoclasts assessed the digestion and remodeling of the cartilage matrix at the bone-cartilage interface (TRACP staining insert in J). (K) Implants including Shh-activated engineered vasculature formed more bone osteoids as compared to the control (planar sections of the implants, paired Student *T*-Test, $n = 5$, $p = 0.003$). D, G, I are consecutive sections from the same implant (group 4). Errors bars are S.D. Scale bars are 500 μ m (D, G, I) and 200 μ m (E, H, J).

(Fig. 4 D, G, and J). The peripheral part of the implants included large osteoids of woven bone (green staining, Fig. 4G) including red, freshly secreted, unmineralized matrix (Fig. 4H). Osteoids partly aligned the osteoinductive particles and included osteoclasts as expected during local IO (27). During EO, the cartilage matrix is remodeled via a digestion by osteoclasts (bone-resorbing cells). We observed lines of tartrate-resistant acid phosphatase (TRACP-) positive osteoclasts at the bone-cartilage interface (Inset, Fig. 4J). We observed Lamellar bone using polarized light (Fig. S6). These results demonstrate that implants recapitulated both IO and EO with the intermediate production of hypertrophic cartilage including collagen type X, the digestion and remodeling of the cartilage by osteoclasts. We speculate that, as previously demonstrated (1, 4), the newly formed osteoids originate from the differentiation of implanted hMSC and from mesenchymal cells from adjacent, injured connective tissue (i.e., muscle).

Contribution of the Engineered Vasculature to the Formation of Immature Skeletal Tissues in Vivo. We quantified the amount of cartilage tissue and bone osteoids formed after 5 weeks of implantation. The cartilage tissue covered between 5 and 25% of the implant area (Alcian blue positive, Fig. 4F). Bone osteoids covered 41% of the implant area in the control group (Group 1), 45% upon treatment with Shh (Group 2, paired Student *T*-Test, $n = 5$, n.s. $p = 0.36$), 49% in implants including an engineered vasculature (Group 3, n.s. $p = 0.2$) and 50% in implants including a Shh-activated engineered vasculature (Group 4, $p = 0.003$, Fig. 4K). Implants without cells did not form any bone. Besides a significant increase in osteoids formation in group 4 vs. group 1,

the synergetic effect of huVEC and Shh did not improve the formation of immature bone as compared to huVEC or Shh alone (group 4 vs. group 2 and 3). We concluded that the in vitro development of the vasculature did not improve the formation of immature bone osteoids.

The Implant Matures into a Bone Organ. To test the effect of in vitro vascular development on the formation of mature bone, we analyzed implants 8 weeks after implantation. Mature bone formed which was structurally similar to normal bones with regions of compact and interconnected trabecular structures (Fig. 5A). Very little cartilage tissue was found after 8 weeks (Fig. 5B, black arrow head) which was again aligning the newly formed bone (Fig. 5B, white arrow head). These observations suggest the completion of the process of EO. Bone was mineralized, had blood vessels (Fig. 5C, black arrow) and bone surface lining osteoblasts synthesizing lamellar bone (Fig. 5C, white arrow). Bone lacunae formed in 4/6 mice which were phenotypically similar to bone-marrow cavities (Fig. 5C, black arrow). The formation of bone-marrow cavities was previously described as related to EO (29). We concluded that the implants recapitulated some aspects of endochondral bone repair leading to the formation of mature bone and contained elements which might initiate the formation of an ectopic bone-marrow cavity.

Contribution of the Engineered Vasculature to the Formation of Mature Bone Tissue in Vivo. We quantified the amount of mature, mineralized bone (cross-sections, basic fuchsin staining Fig. 5E–H, 5 mice). Implants including a Shh-activated engineered vascu-

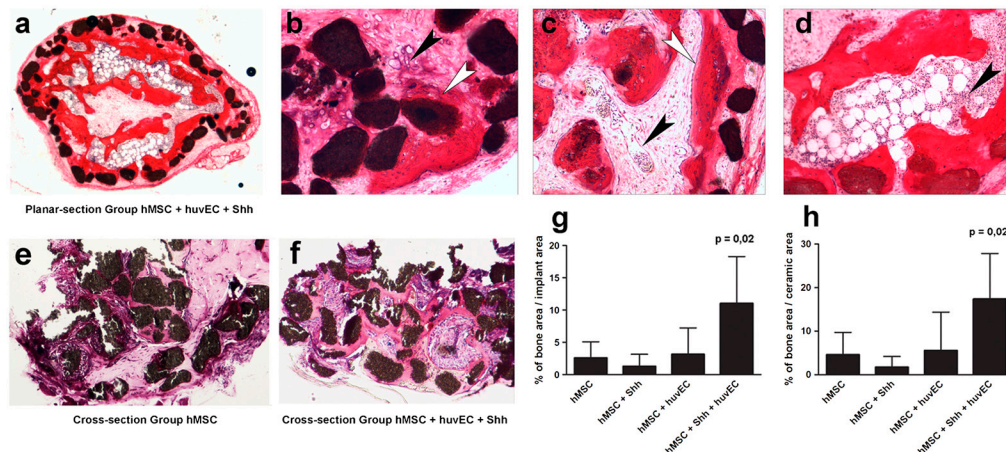


Fig. 5. Solely implants including a Shh-activated engineered vasculature enhance the formation of mature bone tissue. (A–D) Implants (same four groups as in Fig. 4) were placed subcutaneously in mice, explanted after 8 weeks, and analyzed for the formation of mature bone. (A–D) Planar sections (10 μ m-thick, basic fuchsin staining) revealed the formation of trabecular-like bone structures (A). Small amount of cartilage (B, black arrow) was aligning areas of mature bone (B, white arrow). The mature bone included bone lining cells (C, white arrow) and blood vessels (C, black arrow). Bone lacunae formed which were filled with a tissue phenotypically similar to bone marrow (D, black arrow). (E–H) Implant with a Shh-activated vasculature included a larger area of mature bone as compared to implants with hMSC alone, hMSC treated with Shh or hMSC and huVEC (G, 4.2 fold, 7 μ m-thick cross-sections of the implants, basic fuchsin staining, paired Student *T*-Test, $n = 5$, $p = 0.02$ (D). A similar increase in mature bone formation was observed upon normalization to the area covered by ceramic scaffolds (H, 3.8 fold, paired Student *T*-Test, $n = 5$, $p = 0.02$). Errors bars are S.D.

lature (group 4) were filled with significantly more bone as compared to the control group (11% of implant area in group 4 vs. 2.6% in group 1, $p = 0.02$, paired student *T*-Test, $n = 5$). Implants in groups 2 and 3 formed similar amounts of mature bone as compared to the control group (1.3% in group 2; 3.1% in group 3). To confirm these results, we normalized the area of bone to the area of the ceramic scaffold. The normalized area of bone formed in group 4 was again significantly higher than in the control group (17.4% for group 4 vs. 4.6% for group 1, $p = 0.02$, paired Student *T*-Test, $n = 5$). One mouse which did not form bone in the group 1 (control group) formed bone in group 4 (Shh-activated engineered blood vessels). These results suggest that the *in vitro* development of engineered blood vessels is necessary to contribute to and enhance the formation of mature bone tissue *in vivo*. Engineered blood vessels in an earlier developmental state fail to contribute to the formation of new mature bone tissue.

Discussion

Bone is one of the few tissues which have the potential to fully repair (1). However, the rapid regeneration of large defects is still very challenging (30). Currently, cell-based therapies exploit the process of intramembranous ossification, rely on a large amount of filling biomaterial to stabilize the wound, are limited in size by delayed vascularization (5, 31), and fail in human clinical applications (30). Here, we hypothesize that such limitations can be circumvented by mimicking endochondral bone repair, a stepwise differentiation of a highly vascularized tissue into cartilage and bone. In recent evidences, we showed that an engineered vasculature can contribute to the vascularization and survival of an implant (6, 19). Here, we demonstrate that the developmental progression of engineered blood vessels (*i*) is modulated by the endogenous and exogenous Hh signaling (vascular lumens number, size, and size distribution), (*ii*) enhances tissue perfusion *in vivo*, and (*iii*) is necessary to contribute to and enhance the formation of mature bone tissue *in vivo*. The regulation of two Hh canonical inhibitors (GAS1 and RAB23) upon Hh inhibition along with the effect of the Smo activator Purmorphamine both argue for a contribution of the canonical pathway to lumen formation. This effect might result from a direct regulation of endothelial cell morphology through the modulation of actin stress fibers (32) and from the production of angiogenic molecules in interstitial cells (11).

This study suggests that the *in vitro* development of engineered vasculatures leads to a more functional, stable vasculature *in vivo*. The density of lumens formed *in vitro* correlated with the density of lumen perfused *in vivo*. In addition, nonlumenized, cord-like structures, formed *in vitro* were absent after explantation. We speculate that the rapid perfusion of the engineered vessels by the blood flow induces a selection and maintenance of the lumenized capillaries while nonperfused cord-like structures progressively regress.

The regenerating callus is highly vascularized (2). In this study, solely implants including a Shh-activated vasculature contributed to and enhanced the formation of mature bone tissue. Besides its classical role in improving oxygen, nutrients, and ions exchanges, the vasculature plays an inductive role. Molecules including VEGF and Hypoxia-inducible factors (HIF1a, HIF2a) directly contribute to chondrocytes survival (33), chondrocytes hypertrophy (34), and osteoblast differentiation (35). Concomitantly, the vasculature recruits osteoclasts, mesenchymal and hematopoietic progenitors to the bone-forming sites and seed the hematopoietic niche (1). We speculate the increased bone formation results from a combination of improved mass transport (*i.e.* oxygen, cells, ions) and vascular inductive function.

We observe the remodeling of a vascularized implant through a combination of intramembranous and endochondral ossification. This implant closely mimicks the natural regenerative process of bone (1). This procedure is clinically relevant, using human adult stem cells in serum-free condition. The use of alternative sources of endothelial cells was previously investigated by us (20). In further investigations, this protocol shall be tested in mechanically challenged orthotopic sites. We hypothesize that the remodeling of the implant through a fibrocartilagenous phase might demonstrate improved compliance to stabilize the fracture, resist mechanical deformation and solicitations using less biomaterial.

We propose that Shh promotes the *in vitro* development of an engineered vasculature whose developmental state determines its *in vivo* contribution to the formation of mature bone. Due to pleiotropic roles of the vasculature in tissue development and tissue function, we believe cell-based therapies will strongly benefit from engineered vasculatures.

Material and Methods

Bone marrow aspirates were obtained from donors with written informed consent. hMSCs were isolated and proliferated as described previously (3). Alternatively, hMSC were obtained from Lonza (Lonza Group Ltd.). Human umbilical vein endothelial cells (hUVECs) were purchased from Lonza (Lonza Group Ltd.). Coculture of hMSC (92%) and hUVEC (8%) were previously optimized (19–20) and obtained by resuspending a total of 150,000 cells per spherical aggregate in 2 mL of differentiation medium and seeded in a well of a Deepwell 96 well-plate (Nunc). The plate was inverted to form a drop hanging from each well. Recombinant human Sonic Hedgehog N-terminus (20 kDa) in 0.1% BSA was supplemented to the culture medium at described physiological concentrations ranging from 0.5 to 30 nM. To eval-

uate the effect of prevascularization and Shh on ectopic bone formation by hMSCs and hUVEC, spherical aggregates (1,500,000 cells/implant). were pooled with osteoinductive biphasic calcium phosphate (BCP) ceramic granules of 100 μ m prepared and sintered at 1,150 °C as described previously (36) and incorporated in 300 μ L of 2 mg/mL rat tail collagen (BD Bioscience). Implants were subcutaneously implanted in immunodeficient mice (Hsd-cpb:NMRI-nu; Harlan) for 5 and 8 weeks. All experiments were approved by the local Animal Experimental Committee. The resulting tissues were evaluated through microarray, PCR, histology, and immunohistochemistry as described in the supplementary data. A detailed description of all material and methods is included in the *SI Text*.

1. Shapiro F (2008) Bone development and its relation to fracture repair. The role of mesenchymal osteoblasts and surface osteoblasts. *Eur Cell Mater* 15:53–76.
2. Glowacki J (1998) Angiogenesis in fracture repair. *Clin Orthop Relat Res* 355S:582–89.
3. Siddappa R, et al. (2008) cAMP/PKA pathway activation in human mesenchymal stem cells in vitro results in robust bone formation in vivo. *Proc Natl Acad Sci USA* 105:7281–7286.
4. Scotti C, et al. (2010) Recapitulation of endochondral bone formation using human adult mesenchymal stem cells as a paradigm for developmental engineering. *Proc Natl Acad Sci USA* 107:7251–7256.
5. Rivron NC, Liu JJ, Rouwkema J, de Boer J, van Blitterswijk CA (2008) Engineering vascularised tissues in vitro. *Eur Cell Mater* 15:27–40.
6. Levenberg S, et al. (2005) Engineering vascularized skeletal muscle tissue. *Nat Biotechnol* 23:879–884.
7. Au P, Tam J, Fukumura D, Jain RK (2008) Bone marrow-derived mesenchymal stem cells facilitate engineering of long-lasting functional vasculature. *Blood* 111:4551–4558.
8. Koike N, et al. (2004) Tissue engineering: Creation of long-lasting blood vessels. *Nature* 428:138–139.
9. Koffler J, et al. (2011) Improved vascular organization enhances functional integration of engineered skeletal muscle grafts. *Proc Natl Acad Sci USA* 108(36):14789–14794.
10. Murakami S, Noda M (2000) Expression of Indian hedgehog during fracture healing in adult rat femora. *Calcif Tissue Int* 66:272–276.
11. Pola R, et al. (2001) The morphogen Sonic hedgehog is an indirect angiogenic agent upregulating two families of angiogenic growth factors. *Nat Med* 7:706–711.
12. Pola R, et al. (2003) Postnatal recapitulation of embryonic hedgehog pathway in response to skeletal muscle ischemia. *Circulation* 108:479–485.
13. Le H, et al. (2008) Hedgehog signaling is essential for normal wound healing. *Wound Repair Regen* 16:768–773.
14. Kusano KF, et al. (2005) Sonic hedgehog myocardial gene therapy: tissue repair through transient reconstitution of embryonic signaling. *Nat Med* 11:1197–1204.
15. Emans PJ, et al. (2007) A novel in vivo model to study endochondral bone formation; HIF-1 α activation and BMP expression. *Bone* 40:409–418.
16. Vokes SA, et al. (2004) Hedgehog signaling is essential for endothelial tube formation during vasculogenesis. *Development* 131:4371–4380.
17. Straface G, et al. (2008) Sonic Hedgehog regulates angiogenesis and myogenesis during post-natal skeletal muscle regeneration. *J Cell Mol Med* 13:2424–2435.
18. Asai J, et al. (2006) Topical sonic hedgehog gene therapy accelerates wound healing in diabetes by enhancing endothelial progenitor cell-mediated microvascular remodeling. *Circulation* 113:2413–2424.
19. Rouwkema J, de Boer J, Van Blitterswijk CA (2006) Endothelial cells assemble into a 3-dimensional prevascular network in a bone tissue engineering construct. *Tissue Eng* 12:2685–2693.
20. Rouwkema J, Westerweel PE, de Boer J, Verhaar MC, van Blitterswijk CA (2009) The use of endothelial progenitor cells for prevascularized bone tissue engineering. *Tissue Eng Part A* 15:2015–2027.
21. Taipale J, et al. (2000) Effects of oncogenic mutations in Smoothed and Patched can be reversed by cyclopamine. *Nature* 406:1005–1009.
22. Iruela-Arispe ML, Davis GE (2009) Cellular and molecular mechanisms of vascular lumen formation. *Dev Cell* 16:222–231.
23. Dessaud E, et al. (2007) Interpretation of the sonic hedgehog morphogen gradient by a temporal adaptation mechanism. *Nature* 450:717–720.
24. Sinha S, Chen JK (2006) Purmorphamine activates the Hedgehog pathway by targeting Smoothed. *Nat Chem Biol* 2:29–30.
25. Muller G, Behrens J, Nussbaumer U, Bohlen P, Birchmeier W (1987) Inhibitory action of transforming growth factor beta on endothelial cells. *Proc Natl Acad Sci USA* 84:5600–5604.
26. Korff T, Kimmina S, Martiny-Baron G, Augustin HG (2001) Blood vessel maturation in a 3-dimensional spheroidal coculture model: direct contact with smooth muscle cells regulates endothelial cell quiescence and abrogates VEGF responsiveness. *FASEB J* 15:447–457.
27. Yuan H, et al. (1998) Osteoinduction by calcium phosphate biomaterials. *J Mater Sci Mater Med* 9:723–726.
28. Armulik A, Abramsson A, Betsholtz C (2005) Endothelial/pericyte interactions. *Circ Res* 97:512–523.
29. Chan CK, et al. (2009) Endochondral ossification is required for haematopoietic stem-cell niche formation. *Nature* 457:490–494.
30. Meijer GJ, de Bruijn JD, Koole R, van Blitterswijk CA (2007) Cell-based bone tissue engineering. *PLoS Med* 4:e9.
31. Rouwkema J, Rivron NC, van Blitterswijk CA (2008) Vascularization in tissue engineering. *Trends Biotechnol* 26:434–441.
32. Chinchilla P, Xiao L, Kazanietz MG, Natalia AN, Riobo GM (2010) Hedgehog proteins activate pro-angiogenic responses in endothelial cells through non-canonical signaling pathways. *Cell Cycle* 9:570–579.
33. Zelzer E, et al. (2004) VEGFA is necessary for chondrocyte survival during bone development. *Development* 131:2161–2171.
34. Wan C, et al. (2010) Role of HIF-1 α in skeletal development. *Ann NY Acad Sci* 1192:322–326.
35. Villars F, et al. (2002) Effect of HUVEC on human osteoprogenitor cell differentiation needs heterotypic gap junction communication. *Am J Physiol Cell Physiol* 282: C775–785.
36. Yuan H, van Blitterswijk CA, de Groot K, de Bruijn JD (2006) Cross-species comparison of ectopic bone formation in biphasic calcium phosphate (BCP) and hydroxyapatite (HA) scaffolds. *Tissue Eng* 12:1607–1615.